A Model for DNA Detection by Metal-Enhanced Fluorescence from Immobilized Silver Nanoparticles on Solid Substrate

Jian Zhang and Joseph R. Lakowicz*

Center for Fluorescence Spectroscopy, University of Maryland School of Medicine, Department of Biochemistry and Molecular Biology, 725 West Lombard Street, Baltimore, Maryland 21201

Received: September 21, 2005; In Final Form: November 14, 2005

N-(2-Mercaptopropionyl)glycine (tiopronin)-coated silver nanoparticles (average diameter of metal core = 5 nm) were prepared by a modified Brust method. Tiopronin ligands were partially displaced by thiolate single-stranded oligonucleotides via ligand exchange. These particles were immobilized onto a solid substrate through hybridization with target oligonucleotides in a layer-by-layer approach. The dye-labeled complementary oligonucleotides were bound to the particle layers through hybridization. Fluorescence intensity was enhanced with a simultaneous increase of plasmon absorbance from accumulated particles. A steady state was shown at the 10th particle layer and then the fluorescence enhancement showed a plateau. This result reveals that increasing the particle layer contributes to fluorescence enhancement. This novel method was used to detect DNA hybridization through both absorbance and emission spectral changes.

Introduction

In the early 1970s, Drexhage et al. found that a fluorophore near a metal film shows a dependence of its emissive lifetime on its distance from the metal surface.[1] Since then, the influence of a metal on the emission of an oscillating dipole has been a subject of considerable theoretical[2] and experimental efforts.[3] It has been proved that fluorescence can be quenched when the fluorophore is in close proximity to a metal particle, but enhanced when the fluorophore is localized at a certain distance.[4,5] Such fluorescence enhancement by metal particle is defined as metal-enhanced fluorescence (MEF) and is applied to increase the sensitivity of target molecule detection in biological assays.[6,7] MEF is believed to occur due to a coupling of the fluorophore with the plasmon resonance from a metal particle, and the enhancement scale depends on the particle size and shape.[8] Our recent model reveals that metal particles contributed to MEF in two ways: an absorption component and a scattering component.[4a] Examinations from Mie theory show that the absorption component that causes fluorescence quenching is the dominant factor for the small particle, while the scattering component that causes fluorescence enhancement is the dominant factor for the large particle.[4a] This model has been confirmed by our experimental results both in solution[9a] and on solid substrates.[9b] Meanwhile, MEF is observed to occur efficiently only when the fluorophore is approximately 10−20 nm from the metal with the island films generated by chemical reduction[10] or vapor deposition.[9b]

The plasmon resonance of a metal particle represents the existence of an electromagnetic field near the metal particle. MEF is caused by increasing the excitation and emission rate of the fluorophore in a localized electromagnetic field.[4,11−13] When the metal particles are in close proximity to each other, the localized electromagnetic fields from individual particles are expected to overlap and result in a denser overlapped field. Fluorescence is enhanced more efficiently when the fluorophore is localized in such an overlapped field.[4a,14] This principle has been applied in biopolymer detections such as DNA[9a] and polysaccharide.[15] However, all these experiments were performed in solution, where the metal particles were dispersed and aggregated randomly. It is of great interest to develop an approach to control the aggregation of the metal particles in order to investigate the dependence of fluorescence enhancement.

Organic monolayer-protected metallic nanoparticles were utilized in this study because of their easily controlled metal core size as well as their versatile and quantitative functionalization through ligand exchange (Scheme 1).[16−18] *N*-(2-Mercaptopropionyl)glycine (abbreviated as tiopronin) was used as ligand, and tiopronin-coated particles displayed chemical stability and solubility in water.[19,20] The silver particles were synthesized with a specific mole ratio of silver salt/tiopronin, and the average diameter of metal core was 5 nm. This type of silver particle was shown to produce only a weak fluorescence enhancement in solution,[9a] so the florescence signal change can be surely ascribable to the coupling of particles when they were immobilized in order on the solid substrate. Thiolate single-stranded oligonucleotides were quantitatively bound to the particles through ligand exchange. These oligonucleotide-displaced particles were immobilized layer-by-layer through hybridization with target oligonucleotides on solid substrate (Scheme 2).[21,22] Dye-labeled oligonucleotides were finally bound to the particle layers through hybridization with the residual single-strand oligonucleotides on the immobilized particles. Dependence of fluorescence signal on the number of particle layer was investigated to compare with the plasmon absorbance change from the immobilized metal particles.

Experimental Section

All reagents and spectroscopic grade solvents were used as received from Fisher or Aldrich. Succinimidyl biotin and egg white avidin were purchased from Sigma. Oligonucleotides (Scheme 3) including TAMRA-labeled oligonucleotide were synthesized by the Biopolymer Laboratory in the University of Maryland at Baltimore. RC dialysis membrane (MWCO 50 000) was purchased from Spectrum Laboratories, Inc. Nanopure water

10.1021/jp055370u CCC: $33.50 © 2006 American Chemical Society
Published on Web 01/20/2006

SCHEME 1: Oligonucleotide Displacement on Tiopronin-Coated Silver Particle via Ligand Exchange and Then Dye-Labeled Oligonucleotide Coupling onto the Particle through Hybridization with Bound Oligonucleotide

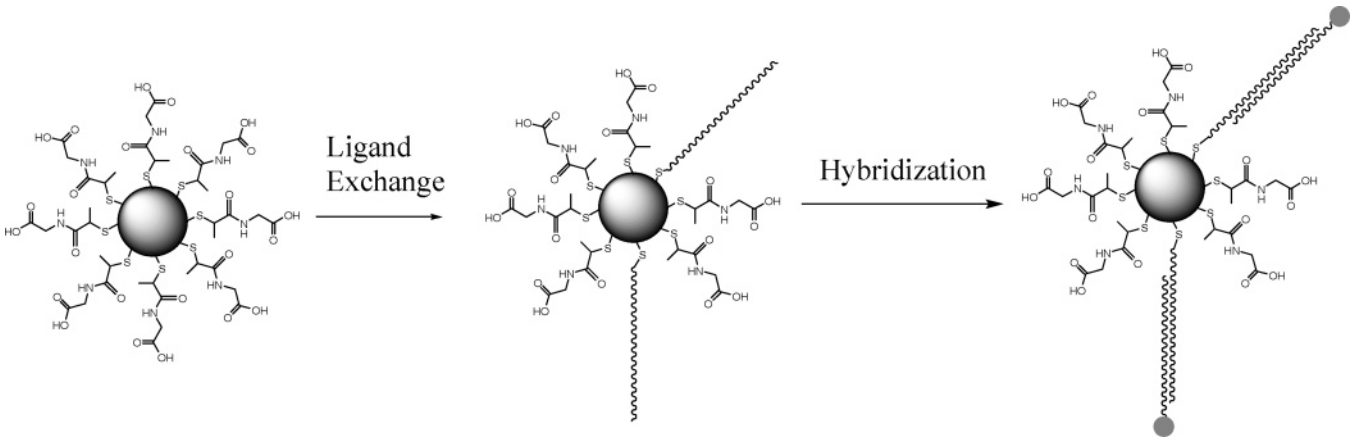

SCHEME 2: A Model for Immobilization of Silver Particles Layer-by-Layer on a Solid Substrate and Labeling with Dye-Labeled Oligonucleotides[a]

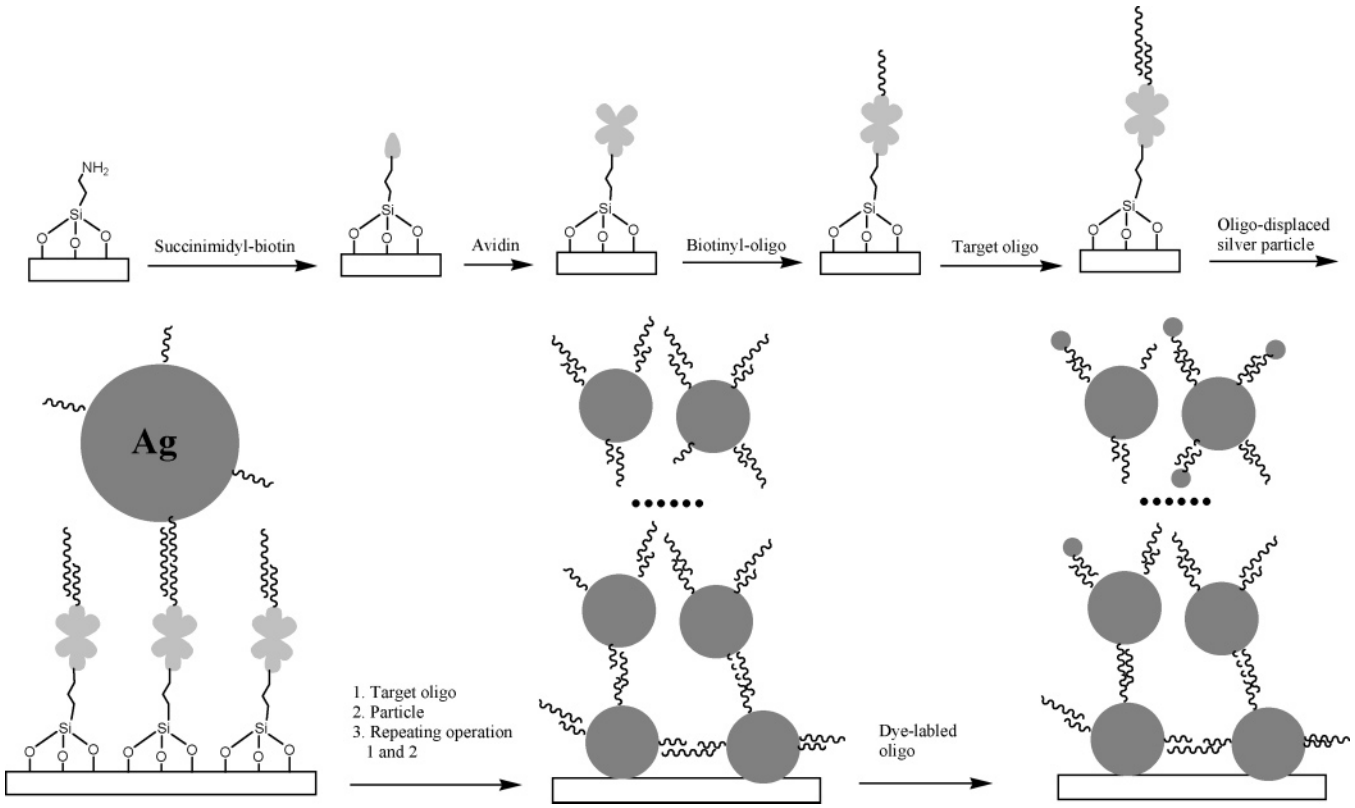

[a] A glass slide was aminated, biotinylated, and avidin-bound, and then biotinylated oligonucleotides were immobilized. Metal particles were immobilized through hybridization with target oligonucleotides onto the solid substrate and then labeled through hybridization with dye-labeled oligonucleotide.

SCHEME 3: Oligonucleotide Structures

1: HS-3′-TCCACACACCACTGGCCATCTTC-5′

2: 3′-AGGTGTGTGGTGACCGGTAGAAG-5′-TAMRA

3: biotin-5′-TCCACACACCACTGGCCATCTTC-3′

4: 3′-AGGTGTGTGGTGACCGGTAGAAGTTTGAAGATGGCCAGTGGTGTGTGGA-5′

(>18.0 MΩ), purified using a Millipore Milli-Q gradient system, was used in all experiments.

Tiopronin−Metal Nanoparticles and Displacement by Thiolate Single-Stranded Oligonucleotide. Tiopronin-coated silver nanoparticles were prepared using a modified Brust reaction with a mole ratio of tiopronin/silver nitrate = 1/2 in methanol using reduction by an excess amount of sodium borohydride.[19,20,23] After removing the solution by filtration, the residual precipitated particles were washed thoroughly with methanol and acetone. Particle (1 mg/mL) and tiopronin (10 mM) were codissolved in water and the solution was stirred for 24 h for annealing of the particles.[25] The water was removed under vacuum and the residue was washed thoroughly with methanol and acetone. The tiopronin-coated particles (particles **1**) were further purified by dissolving in water and dialyzing against water.

The tiopronin ligands on the metal particle were displaced partially by thiolate single-stranded oligonucleotides (oligo-**1** in Scheme 3) through ligand exchange in water with a mole

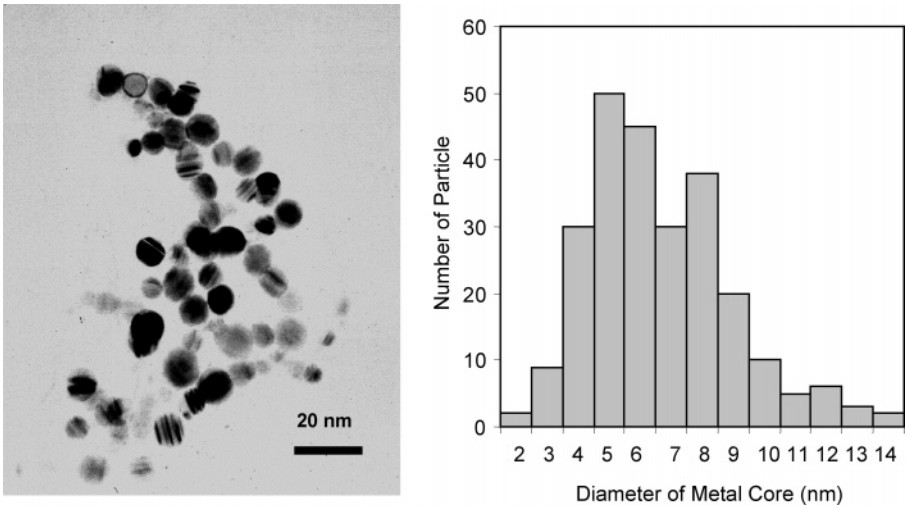

Figure 1. TEM images and histogram of oligonucleotide-displaced silver particle.

ratios of oligonucleotide/tiopronin = 1/1 for 72 h at room temperature.[26] Unbound oligonucleotides were removed by dialysis against water to obtain oligo-displaced particles (particles **2**). Oligo-**1** on the particles (1 mg/mL) were coupled by dye-labeled oligonucleotide (oligo-**2**, 1×10^{-4} M) through hybridization in 10 mM NaCl solution at pH = 7.4 for 24 h, and then the unbound oligo-**2** was removed through dialysis against water to obtain the dye-labeled particles (particles **3**).

Immobilization of Metal Particles on Solid Substrate. The particles were immobilized on the solid substrate in a layer-by-layer method (Scheme 2). To bind the oligonucleotides on the surface,[11] the glass slides were cleaned in a mixture of H_2SO_4/H_2O_2 (v/v = 7/3) for 24 h and then rinsed thoroughly with water, acetone, and ethanol, respectively. The slide surfaces were aminated in a 10 mM 3-aminopropyltrimethylsilane ethanol solution for 12 h. Biotin molecules were bound to the surfaces by incubating the slide in the succinimidyl biotin aqueous solution (1.0 mM) for 12 h. The biotinylated slides were then incubated in avidin buffer solution (avidin = 0.1 mg/mL in 0.1 M NaCl, pH = 7.4) for 12 h to absorb the avidin. Biotinyl-oligonucleotides (oligo-**3**) were bound to the solid substrate through interaction with avidin on the surface in buffer solution (oligo-**3** = 1×10^{-8} M in 0.1 M NaCl, pH = 7.4). Target oligonucleotides (oligo-**4**) were hybridized with oligo-**3** on the solid substrate from buffer solution (oligo-**4** = 1×10^{-7} M in 0.1 M NaCl, pH = 7.4).[9] The particles **2** were immobilized onto the solid substrate through hybridization with oligo-**4** on the surface in buffer solution (particle **2** = 0.1 mg/mL in 10 mM NaCl, pH = 7.4). Cyclic operations of binding oligo-**4** and immobilizing particle **2** were repeated as required. The TAMRA-labeled oligo-**2** were bound to the particle layer from buffer solution (oligo-**2** = 1×10^{-8} M in 10 mM NaCl, pH = 7.4) through hybridization with oligo-**1** on immobilized particle **2** and oligo-**3** on the solid substrate for 2 h. Oligo-**2** bound on the solid substrate was measured quantitatively through a change of emission intensity before and after hybridization.

Spectra. Absorption spectra were monitored with a Hewlett-Packard 8453 spectrophotometer. Fluorescence spectra of samples in solution were recorded with a Cary Eclipse fluorescence spectrophotometer. Fluorescence spectra on the surface were recorded on a SLM 8000 spectrofluorometer in front face under excitation at 510 nm with a mode-locked argon ion laser.[11] Samples were excited by a light at a 45° angle and data collected at a right angle. Transmission electron micrographs (TEM) were taken with a side-entry Philips electron microscope at 120 keV. Samples were cast from water solutions onto standard carbon-coated (200−300 Å) Formvar films on copper grids (200 mesh) by placing a droplet of a 1 mg/mL aqueous sample solution on grids. The size distribution of metal core was analyzed with Scion Image Beta Release 2 counting at least 200 particles.

Results and Discussion

Silver nitrate reacted with tiopronin to produce a silver salt that was reduced by sodium borohydride to generate tiopronin-coated particles (particles **1**).[19] The particles **1** were washed with ethanol and acetone thoroughly to remove uncapped thiol and then mildly annealed in a 10 mM tiopronin aqueous solution for 24 h. They were further purified by dialysis against water.[25] The metal cores on these particles were outlined by TEM images (Figure 1), and the size distribution of the metal core was analyzed from at least 200 individual particles. The average core diameter of these particles was estimated to be ~5 nm. Although the particles were annealed, they still displayed polydispersity.[17] The average chemical composition hence was suggested to be $Ag_{4033}(tiopronin)_{453}$ for these particles.[24] The absorbance spectrum displayed a plasmon peak at 415 nm in water (Figure 2), consistent with our previous result for this type of silver particle.[26]

Thiolate single-stranded oligonucleotides (oligo-**1**) were quantitatively displaced on the defect sites of metal cores (edges and vertexes) of the particles **1** through a ligand exchange reaction.[25,26] These oligo-bound silver particles (particles **2**) were immobilized onto the solid substrates. The particle **2** displayed a plasmon wavelength at 406 nm (Figure 2), 9 nm blue-shifted as compared to the particle **1**. Oligo-**1** on the particles **2** were hybridized with dye-labeled oligo-**2** to obtain the dye-labeled particle (particle **3**), but the hybridization did not produce a detectable absorbance spectral change. Oligo-**2** on the particle **3** exhibited an emission maximum at 586 nm upon excitation at 510 nm (Figure 2), 5 nm red-shifting from free oligo-**2** in water, revealing that the hybridization between oligo-**1** on the particle **2** and oligo-**2** in solution could occur efficiently.

The quantity of oligonucleotide capped on the particles was estimated from the emission intensity by a standard linear calibration curve.[27] A cyanide solution was used to dissolve the silver core and release the ligands into solution.[28] Standard curves were measured with known concentrations of dye-labeled oligonucleotide using identical amounts of buffer solution and cyanide concentration. Because the dye-labeled oligonucleotides

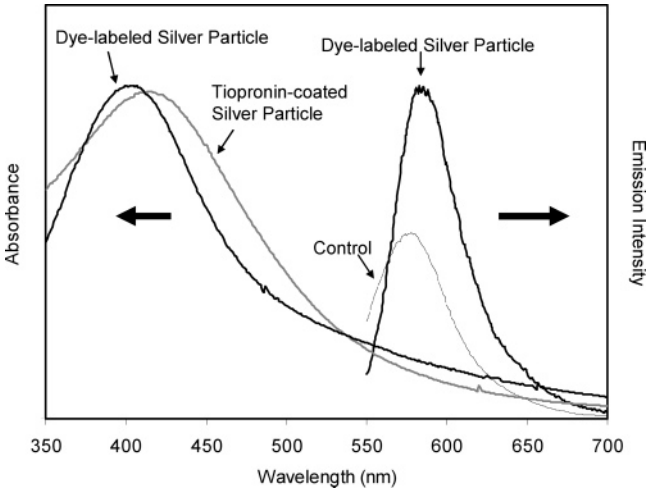

Figure 2. Absorbance spectra of tiopronin-coated silver particle and oligonucleotide-displaced silver particle (concentration = 6.1×10^{-7} M) and emission spectra of dye-labeled oligonucleotide hybridized particle (concentration = 6.1×10^{-7} M) and control (concentration = 7.3×10^{-6} M for the dye-labeled oligo and concentration = 6.1×10^{-7} M for the tiopronin-coated particle) upon excitation at 510 nm in buffer.

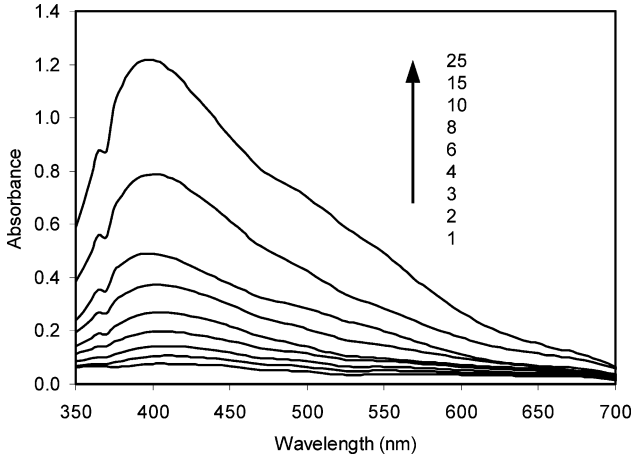

Figure 3. Absorbance spectral change from immobilized silver particles upon increasing the particle layer number on solid substrate.

TABLE 1: Dependence of Surface Concentration of Dye-Labeled Oligo-2 on the Particle Layers Immobilized onto the Solid Substrate

layer number	0	1	2	3	4	6	8	10	15	25
coverage × 10^{12} mol/cm^2	2	0.9	0.7	0.6	0.7	0.8	1.0	0.9	0.9	1.0

were in excess in solution, all oligo-**1** on the particles were expected to hybridize with dye-labeled oligo-**2**. When the metal cores were removed by cyanide in solution, the emission maximum was converted to the molar concentration of oligonucleotide by interpolation from a standard linear calibration curve. From the concentrations of oligonucleotide and particle, it was estimated that the composition of oligonucleotide-displaced particle was $Ag_{4033}(ligand)_{445}(oligo)_{12}$. Using a mixture of dye-labeled oligo-**2** and particle **1** with the same concentrations as the control, the emission was enhanced only 1.6-fold (Figure 2), indicating that the fluorescence could not be enhanced efficiently on the individual particles of this size. This value was also analogous to our previous result from cyanine-labeled oligonucleotide on a silver particle with the same metal particle size.[9a]

To immobilize the particles **2** onto the solid substrates, the glass slides were first aminated with 3-aminopropyltrimethylsilane (Scheme 2) and then biotinylated by condensation between the amino group on the slides and succinimidyl biotin in solution. Avidin molecules were bound to the solid substrate through interaction with immobilized biotin, and then biotinylated oligonucleotides (oligo-**3**) were bound through interaction with the avidin. The target oligonucleotides (oligo-**4**) were coupled through hybridization with immobilized oligo-**3** on the surface. The particles **2** were immobilized through hybridization between the oligo-**1** on the particle **2** and target oligo-**4** on the surface. Multiple particle layers were formed by repetition of hybridization between oligo-**4** and particle **2**.

The immobilization of particles was verified by the plasmon absorbance increasing at 400 nm with the repeated operations (Figure 3).[22] This wavelength was 6 nm blue-shifted as compared with that of free particle in solution. An analogous observation was reported by Ozaki,[29] probably due to an environmental change near the silver particles. The absorbance intensity increased proportionally with the number of repetitive operations, suggesting that one particle layer consumed in a close quantity of particle when forming such a layer-by-layer particle structure. Each operation resulted in 0.05 of absorbance increase at 400 nm. When the extinction coefficient at the plasmon wavelength was 6.5×10^5 cm^{-1} M^{-1}, the thickness of the immobilized particle layer was estimated to be 20 nm for each operation. This value was close to the out-spherical diameter of particle **2** including to two oligo-**1** lengths (8 nm) and one metal core diameter (5 nm), so we proposed that only one layer of particle was immobilized in each treatment under the current conditions. It was noted that the particles were immobilized on the solid substrate as only a single layer in each immobilization treatment, different from the results using other immobilization media.[30] We ascribed it to a relatively low quantity of oligonucleotide on each particle as well as the weak binding of metal particle through the DNA hybridization in this study. The absorbance wavelength from the immobilized metal particle herein was almost independent of the particle layer, which was probably due to a large interparticle spacing (>2.5 times larger than the diameter of particle), which led to an almost negligible wavelength red-shifting effect.[31,32]

We are interested in the dependence of fluorescence from bound dye-labeled oligo-**2** on the layer number of immobilized particle on solid substrate, so it is important to carefully bind the dye-labeled oligonucleotides with similar surface concentration. To achieve this, oligo-**2** had the same concentration (1×10^{-8} M) in buffer solution and short incubating time. The quantity of bound oligo-**2** was estimated from an emission decrease before and after hybridization due to the decrease in the amount of oligo-**2** in solution. It was shown that the coverage was $(8 \pm 2) \times 10^{-13}$ mol/cm^2 (Table 1), which was almost independent of the layer number. It was difficult to distinguish the localization of oligo-**2** on the particle layers, although they were supposed to interact more easily with oligo-**1** on the top layer than those beneath the top layer because of steric hindrance. But it was supposed that there still may be some oligo-**2** localized beneath the top particle layer.

The coverage of oligo-**2** on the blank substrate was estimated to be 2×10^{-12} mol/cm^2, 2-fold higher than that on the particle layer, which was probably due to the higher density of oligo-**3** on the blank substrate. The emission was normalized by multiplying with 0.4 to use as the control in this study. Oligo-**2** on the solid substrate displayed an emission maximum at 567 nm upon excitation at 510 nm (Figure 4), 14 nm blue-shifted from unbound oligo-**2** in solution. The reflection and/or scattering of the excitation light by the accumulated nanoparticle

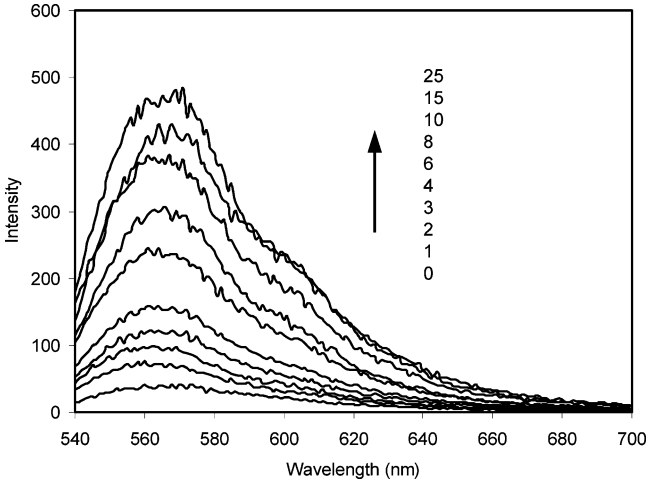

Figure 4. Emission spectral change from dye-labeled oligonucleotide bound onto the particle layers upon increasing the particle layer number on solid substrate with excitation at 510 nm. The spectra were normalized by the concentrations of dye-labeled oligonucleotide on the solid substrate.

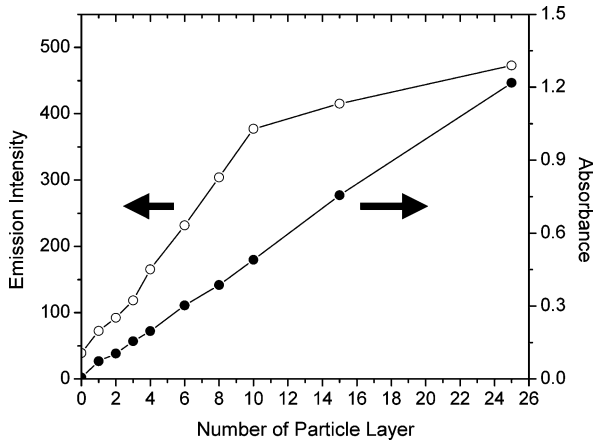

Figure 5. Dependence of absorbance at 400 nm and emission at 567 nm upon excitation at 510 nm on the particle layer number.

layers could contribute to the apparent emission spectrum. However, all these samples are optically thin, so this effect seems to be minor. To confirm this viewpoint, the emission backgrounds were measured from the corresponding silver particle layers coated on the glass slides prior to dye binding and subtracted from the emission spectra of immobilized dye. These backgrounds were found to be less than 6% of the corresponding apparent emission spectra, implying that the contributions from multiple reflections and scattering had been reduced to a very low level after such treatments. There is a most probable fluorophore−plasmon coupling contribution to the emission increase, and this fact is demonstrated in the experiments.

The fluorescence spectra were normalized to the coverage of oligo-**2** to 8×10^{-13} mol/cm^2 (Figure 4). It was shown that the emission wavelength did not significantly change, but the intensity was enhanced by increasing the particle layers. Hence, the particle accumulation on the solid substrate can lead to both increases of absorbance (Figure 3) and emission (Figure 4). To compare the similarity and difference of these two spectral changes, both the absorbance at 400 nm and emission at 567 nm were plotted against the layer number (Figure 5). It was shown that both the absorbance and emission increased simultaneously with the particle layer number. However, the emission enhancement reached a plateau at the 10th layer, but the

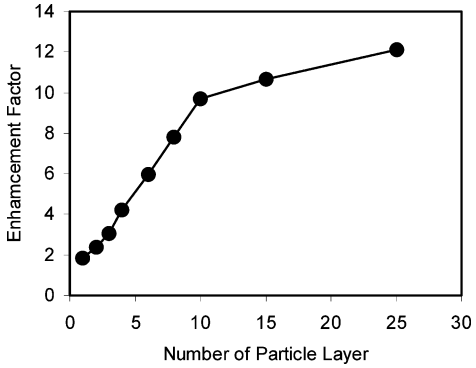

Figure 6. Dependence of enhancement factor of bound oligo-**2** on the particle layer number.

absorbance still increased proportionally. Using the emission intensity on the blank substrate as the control, the enhancement factor, which was calculated from the emission intensity at 567 nm on the particle layer over that on the control, was plotted against the layer number (Figure 6). The enhancement factor increased dramatically at low layer numbers but reached a steady state at the 10th layer.

It was known that oligo-**2** bound at a close coverage on the particle layer for each sample, so the fluorescence enhancement was principally due to the number of immobilized particle layers. The enhancement factor on the first layer was 1.8, close to that of an individual particle in solution, implying that the one-layer metal particle could not induce an effective MEF. The fluorescence was enhanced significantly with the layer number, from 1.8 at the first layer to 10 at the 10th layer. For a sample with multiple particle layers, if the fluorescence enhancement of dye-labeled oligonucleotides on the top layer was close to that on a one layer sample (1.8), its higher enhancement efficiency was due to those dye-labeled oligonucleotides localized beneath the top particle layer. In the other words, more dye-labeled oligonucleotides entered the space between the particle layers to hybridize with unbound oligo-**1** and -**3**, and the coupling of fluorophore and multiply particle layer became more efficient with increasing immobilized particle layer.

The enhancement efficiency of dye on the first layer is below 2, so the enhancement efficiency of the dye beneath the top layer may be much higher than 10 for the 10-layer sample. This value is higher than that obtained on the randomly coupled particles, implying that the enhancement efficiency of dye on the layered coupled particles is higher than that on the randomly coupled particles in solution. Some papers have been published to describe the changes of electromagnetic field with a close proximate of metal particles.[33,34] The situation is more complicated in this study due to multiple couplings of metal particles. The polarization is generally set parallel to the center axis of the particle center, so the coupled particles can be simply regarded to induce an extremely intensive overlapped field on the horizontal direction but a weak field on the vertical direction to the solid substrate. This is perhaps why the dye-labeled oligo on the top layer cannot be enhanced as effectively as those localized beneath the top layer. In addition, the distance between neighboring particle layers is 20 nm, so the dye molecules localized beneath the top layer are about 10 nm from the metal particles, close to the convenient distance of maximum MEF on the metal particles.[9b,11] Hence, the dye-labeled oligonucleotides on the layered coupled particles display an effective fluorescence enhancement in this study.

The plasmon absorbance from the immobilized particle rose proportionally with the layer number while the fluorescence

enhancement began to plateau to its value at 10 layers (Figure 5). The reason is uncertain, but we can attribute this dichotomy to the equilibrium distribution of dye-labeled oligonucleotides on and beneath the top particle layer in the hybridization. Meanwhile, extension of the electromagnetic field through the metal may be different from that through the organic or biological medium.

Conclusions

Fluorescence is enhanced when a dye is localized in an electromagnetic field near a metal surface, and the enhancement becomes stronger in an overlapped electromagnetic field by particle couplings. We have confirmed this prediction using coupled particles in solution. However, such particle coupling is supposed to aggregate randomly in solution. More information can be provided when studying that on orderly coupled particles. The tiopronin-coated silver particles were made with a 5 nm average diameter of the metal core. Thiol single-stranded oligonucleotides were partially displaced on the particles through ligand exchange. The particles were immobilized on the solid substrate through hybridization of oligonucleotides capped on the particles with oligonucleotides on the solid substrate. The particle immobilization treatments were repeated cyclically, resulting in a layer-by-layer increase of the particle on the solid substrate, and the accumulation of the particle layer was verified by a proportional increase of plasmon absorbance from the immobilized particles. Similar to solution, the dye-labeled oligonucleotides were bound to the particle layer through hybridization with the oligonucleotides on the immobilized particles in close surface concentrations. The fluorescence was shown to enhance dramatically with an increase of particle layer until the 10th layer, after which the enhancement began to plateau at the maximal value. This result reveals that the fluorescence enhancement can be used to develop a target DNA detection model parallel to the absorbance rising.

Acknowledgment. This research was supported by a grant from NIH, HG-02655, EB-00682, and NCRR, RR-08119.

References and Notes

(1) (a) Drexhage, K. H. *J. Lumin.* **1970**, *12*, 693. (b) Drexhage, K. H. *Progress in Optics XII*; Wolf, E., Ed.; North Holland: Amsterdam, 1974.

(2) (a) Adams, A.; Rendell, R. W.; Garnett, R. W.; Hansma, P. K.; Metiu, H. *Optics Commun.* **1980**, *34*, 417. (b) Weitz, D. A.; Garoff, S.; Hanson, C. D.; Gramila, T. *J. Opt. Lett.* **1982**, *7*, 89. (c) Leitner, A.; Lippitsch, M. E.; Draxler, S.; Riegler, M.; Aussenegg, F. R. *Appl. Phys. B* **1985**, *36*, 105. (d) Aussenegg, F. R.; Leitner, A.; Lippitsch, M. E.; Reinisch, H.; Riegler, M. *Surf. Sci.* **1987**, *139*, 935. (e) Sokolov, K.; Chumanov, G.; Cotton, T. M. *Anal. Chem.* **1998**, *70*, 3898. (f) Tarcha, P. J.; De Saja-Gonzalez, J.; Rodriguez-Llorente, S.; Aroca, R. *Appl. Spectrosc.* **1999**, *53*, 43. (g) De Saja-Gonzalez, J.; Aroca, R; Nagao, Y.; De Saja, J. A. *Spectrochim. Acta A* **1997**, *53*, 173.

(3) (a) Tews, K. H. *J. Lumin.* **1974**, *9*, 223. (b) Chance, R. R.; Prock, A.; Silbey, R. *J. Chem. Phys.* **1974**, *60*, 2744. (c) Persson, B. N. J. *J. Phys. C Solid State Phys.* **1978**, *11*, 4251. (d) Gersten, J.; Nitzan, A. *J. Chem. Phys.* **1981**, *75*, 1139. (e) Ruppin, R. *J. Chem. Phys.* **1982**, *76*, 1681. (f) Barnes, W. L. *J. Modern Opt.* **1998**, *45*, 661

(4) (a) Lakowicz, J. R. *Anal. Biochem.* **2005**, *337*, 171. (b) Lakowicz, J. R. *Anal. Biochem.* **2001**, *298*, 1.

(5) (a) Kummerlen, J.; Leitner, A.; Brunner, H.; Aussenegg, F. R.; Wokaun, A. *Mol. Phys.* **1993**, *80*, 1031. (b) Sokolov, K.; Chumanov, G.; Cotton, T. M. *Anal. Chem.* **1998**, *70*, 3898. (c) Antunes, P. A.; Constantino, C. J. L., Aroca, R. F., Duff, J. *Langmuir* **2001**, *17*, 2958. (d) Kamat P. V. *J. Phys.* Chem. B **2002**, *106*, 7729. (e) Kulakovich, O.; Strekal, N.; Yaroshevich, A.; Maskevich, S.; Gaponenko, S.; Nabiev, I.; Woggon, U.; Artemyev, M. *Nano Lett.* **2002**, *2*, 1449.

(6) Lakowicz, J. R.; *Emerging Biomedical Application of Time-Resolved Florescence Spectroscopy, Topic in Fluorescence Spectroscopy, Vol 4, Probe Design and Chemical Sensin;,* Lakowicz, J. R., Ed.; Plenum Press: New York, 1994.

(7) (a) *Frontiers in Biosensorics I. Fundamental Aspects*; Scheller, F. W., Schubert, F., Fedrowitz, J., Eds.; Birkhauser Verlag: Berlin, 1997. (b) *Frontiers in Biosensorics II. Practical Applications*; Scheller, F. W., Schubert, F., Fedrowitz, J., Eds.; Birkhauser Verlag: Berlin, 1997.

(8) (a) Kreibig, U.; Vollmer, M. *Optical Properties of Metal Clusters*; Springer-Verlag: Berlin, 1995. (b) Kerker, M.; Blatchford, C. G. *Phys. Rev. B* **1982**, *26*, 4052.

(9) (a) Zhang, J.; Malicka, J.; Gryczynski, I.; Lakowicz, J. R. *J. Phys. Chem. B.* **2005**, *109*, 7643. (b) Zhang, J.; Matveeva, E.; Gryczynski, I.; Leonenko, Z.; Lakowicz, J. R. *J. Phys. Chem. B.* **2005**, *109*, 7969−7975.

(10) Zhang, J.; Lakowicz, J. R. *J. Phys. Chem. B.* **2005**, *109*, 8701.

(11) (a) Malicka, J.; Gryczynski, I.; Gryczynski, Z.; Lakowicz, J. R. *Anal. Biochem.* **2003**, *315*, 57. (b) Malicka, J.; Gryczynski, I.; Fang, J.; Kusba, J.; Lakowicz, J. R. *Anal. Biochem.* **2003**, *315*, 160.

(12) (a) Messinger, B. J.; von Raben, K. U.; Chang, R. K.; Barber, P. W. *Phys. Rev. B* **1981**, *24*, 649. (b) Quinten, M. *Appl. Phys. B: Laser Opt.* **2001**, *73*, 245.

(13) Kneipp, K.; Kneipp, H.; Itzkan, I.; Dasari, D. R.; Feld, M. S. *Chem. Rev.* **1999**, *99*, 2957.

(14) Evanoff, D. D., Jr.; White, R. L.; Chumanov, G. *J. Phys. Chem. B.* **2004**, *108*, 1522.

(15) Zhang, J.; Geddes, C. D.; Lakowicz, J. R. *Anal. Biochem.* **2004**, *332*, 253.

(16) Templeton, A. C.; Wuelfing, W. P.; Murray, R. W. *Acc. Chem. Res.* **2000**, *33*, 27.

(17) (a) Templeton, A. C.; Hostetler, M. J.; Kraft, C. T.; Murray, R. W. *J. Am. Chem. Soc.* **1998**, *120*, 1906. (b) Hostetler, M. J.; Templeton, A. C.; Murray, R. W. *Langmuir* **1999**, *15*, 3782. Hostetler, M. J.; Green, S. J.; Stokes, J. J.; Murray, R. W. *J. Am. Chem. Soc.* **1996**, *118*, 4212.

(18) Ingram, R. S.; Hostetler, M. J.; Murray, R. W. *J. Am. Chem. Soc.* **1997**, *119*, 9175.

(19) Huang, T.; Murray, R. W. *J. Phys. Chem. B* **2001**, *105*, 12498.

(20) Huang, T.; Murray, R. W. *Langmuir* **2002**, *18*, 7077.

(21) (a) Tokareva, I.; Hutter, E. *J. Am. Chem. Soc.* **2004**, *126*, 15784. (b) Cobbe, S.; Connolly, S.; Nagle, L.; Eritja, R.; Fitzmaurice, D.; Ryan, D. *J. Phys. Chem. B.* **2003**, *107*, 470. (c) Li, H.; Rothberg, L. J. *Anal. Chem.* **2004**, *76*, 5414.

(22) (a) Rosi, N. L.; Mirkin, C. A. *Chem. Rev.* **2005**, *105*, 1547. (b) Park, S.-J.; Lazarides, A. A.; Storhoff, J. J.; Pesce, L.; Mirkin, C. A. *J. Phys. Chem. B.* **2004**, *108*, 12375. (c) Jin, R.; Wu, G.; Li, Z.; Mirkin, C. A.; Schatz, G. C. *J. Am. Chem. Soc.* **2003**, *125*, 1643. (d) Storhoff, J. J.; Elghanian, R.; Mirkin, C. A.; Letsinger, R. L. *Langmuir* **2002**, *18*, 6666.

(23) Brust, M.; Walker, M.; Bethell, D.; Schiffrin, D. J.; Whyman, R. *J. Chem. Soc., Chem. Commun.* **1994**, 801.

(24) Hostetler, M. J.; Wingate, J. E.; Zhong, C.-J.; Harris, J. E.; Vachet, R. W.; Clark, M. R.; Londono, J. D.; Green, S. J.; Stokes, J. J.; Wignall, G. D.; Glish, G. L.; Porter, M. D.; Evans, N. D.; Murray, R. W. *Langmuir* **1998**, *14*, 17.

(25) (a) Hicks, J. F.; Miles, D. T.; Murray, R. W. *J. Am. Chem. Soc.* **2002**, *124*, 13322. (b) Schaaff, T. G.; Shafigullin, M. N.; Khoury, J. T. Vezmar, I.; Whetten, R. I. *J. Phys. Chem.* **2001**, *105*, *8785*.

(26) Zhang, J.; Malicka, J.; Gryczynski, I.; Lakowicz, J. R. *Anal. Biochem.* **2004**, *330*, 81.

(27) Zhao, Z.; Shen, T.; Xu, H. *Spectrochim. Acta* **1989**, *45A*, 1113−1116.

(28) (a) Demers, L. M.; Mirkin, C. A.; Mucic, R. C.; Reynolds, R. A., III; Letsinger, R. L.; Elghanian, R.; Viswanadham, G. *Anal. Chem.* **2000**, *72*, 5535. (b) Taton, T. A.; Mucic, R. C.; Mirkin, C. A.; Letsinger, R. L. *J. Am. Chem. Soc.* **2000**, *122*, 6305. (c) Storhoff, J. J.; Lazarides, A. A.; Mirkin, C. A.; Letsinger, R. L.; Mucic, R. C.; Schatz, G. C. *J. Am. Chem. Soc.* **2000**, *122*, 4640−4650. (d) Marinakos, S. M.; Novak, J. P.; Brousseau, L. C.; House, A. B.; Edeki, E. M.; Feldhaus, J. C.; Feldheim, D. C. *J. Am. Chem. Soc.* **1999**, *121*, 8518.

(29) Li, X.; Xu, W.; Zhang, J.; Jia, H.; Yang, B.; Zhao, B.; Li, B.; Ozaki, Y. *Langmuir* **2004** *20*, 1298.

(30) Hicks, J. F.; Seok-Shon, Y.; Murray, R. W. *Langmuir* **2002**, *18*, 2288.

(31) Bouhelier, A.; Bachelot, R.; Im, J. S.; Wiederrecht, G. P.; Lerondel, G.; Kostcheev, S.; Royer, P. *J. Phys. Chem. B* **2005**, *109*, 3195.

(32) Su, K.-H.; Wei, Q.-H.; Zhang, X.; Mock, J. J.; Smith, D. R.; Schultz S. *Nano Lett.* **2003**, *3*, 1087.

(33) (a) Su, K.-H.; Wei, Q.-H.; Zhang, X.; Mock, J. J.; Smith, D. R.; Schultz, S. *Nano Lett.* **2003**, *3*, 1087. (b) Gunnarsson, L.; Rindzevicius, T.; Prikulis, J.; Kasemo, B.; Kall, M.; Zou, S.; Schatz, G. C. *J. Phys. Chem. B* **2005**, *109*, 1079.

(34) (a) Atay, T.; Song, J.-H.; Nurmikko, A. V. *Nano Lett.* **2004**, *4*, 1627. (b) Bouhelier, A.; Bachelot, R.; Im, J. S.; Wiederrecht, G. P.; Lerondel, G.; Kostcheev, S.; Royer, P. *J. Phys. Chem. B.* **2005**, *109*, 3195.